

Semantic Histogram Based Graph Matching for Real-Time Multi-Robot Global Localization in Large Scale Environment*

Xiyue Guo¹, Junjie Hu¹, *Member, IEEE*, Junfeng Chen¹, Fuqin Deng¹,
and Tin Lun Lam^{1,2,†}, *Senior Member, IEEE*

Abstract—The core problem of visual multi-robot simultaneous localization and mapping (MR-SLAM) is how to efficiently and accurately perform multi-robot global localization (MR-GL). The difficulties are two-fold. The first is the difficulty of global localization for significant viewpoint difference. Appearance-based localization methods tend to fail under large viewpoint changes. Recently, semantic graphs have been utilized to overcome the viewpoint variation problem. However, the methods are highly time-consuming, especially in large-scale environments. This leads to the second difficulty, which is how to perform real-time global localization. In this paper, we propose a semantic histogram-based graph matching method that is robust to viewpoint variation and can achieve real-time global localization. Based on that, we develop a system that can accurately and efficiently perform MR-GL for both homogeneous and heterogeneous robots. The experimental results show that our approach is about 30 times faster than Random Walk based semantic descriptors. Moreover, it achieves an accuracy of 95% for global localization, while the accuracy of the state-of-the-art method is 85%.

I. INTRODUCTION

Vision based single-robot simultaneous localization and mapping (SR-SLAM) have gained significant progress over the past decades. However, it has fundamental limitations of mapping speed, mission range, localization accuracy, etc. Thus, it usually performs poorly for large scale environments. To overcome these problems, multi-robot SLAM (MR-SLAM) maps large scale unknown environments by exploiting several collaborating robots. Although it has clear advantages against SR-SLAM with multi-robot cooperation, the preliminary difficulty is that we need the multi-robot global localization to satisfy the requirement of real-world deployment.

There are mainly two difficulties towards achieving this goal. First, an urgent problem is the accurate global localization for the large viewpoint difference between individual robots. It's known that MR-SLAM is applicable for large scale environments. The viewpoint differences between robots are very large. The difference is more significant for heterogeneous robot systems. An example is given in Fig. 1, the images captured by a vehicle show a clear viewpoint difference from those captured by a drone. Second, the global localization has to be computationally efficient; otherwise, the MR-SLAM will collapse.

*This work was partially supported by funding 2019-INT008 from the Shenzhen Institute of Artificial Intelligence and Robotics for Society.

¹The Shenzhen Institute of Artificial Intelligence and Robotics for Society.

²The Chinese University of Hong Kong, Shenzhen.

[†]Corresponding author is Tin Lun Lam tlam@cuhk.edu.cn

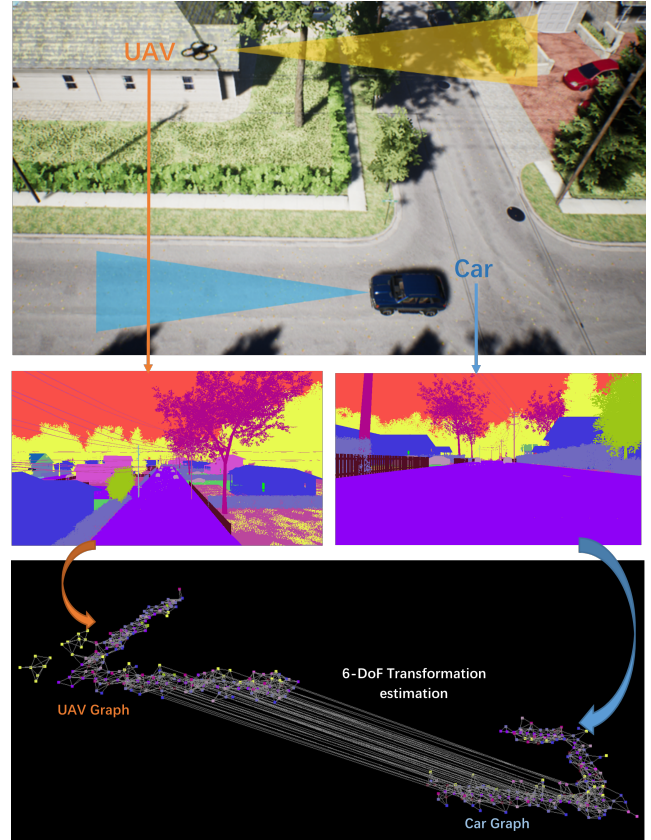


Fig. 1. An example of our semantic based graph matching method. The method is used for global localization in a large scale environment. The viewpoint between two robots (UAV and Car) is extremely large. We utilize semantic maps to build semantic graphs for two robots. Then, the transformation matrix between them can be simply estimated.

In previous studies, traditional appearance-based methods such as the Bag-of-Word (BoW) [1], [2] are the most widely used localization methods for MR-SLAM [3], [4]. However, Under the large viewpoint changes, local image features (e.g. SIFT [5], SURF [6], ORB [7], FAST [8]) will change significantly, this cause appearance-based methods to fail. As semantic information is invariant to the viewpoint changes, recently, several methods [9]–[11] proposed to use semantics for global localization. In these works, semantic-based graphs are first built for different viewpoints, then the different view's graphs are matched by utilizing the semantic information. These methods demonstrate better performance compared with appearance-based methods for large viewpoint changes.

II. RELATED WORK

A. Appearance-based Approaches

Appearance-based localization methods such as Bag-of-Words (Bow) use global or local visual features to find the association of images [5]–[8]. One representative work is FAB-MAP [2]. These methods work well under the small viewpoint difference. However, when the viewpoint difference is large, the localization systems become less reliable.

Recently, convolution neural network (CNNs) has been employed to overcome the viewpoint change problem. In [12], [13], the viewpoint invariant landmarks are generated by CNNs. However, these landmarks are not reliable when the viewpoint change becomes significant (e.g., opposite direction, viewpoint changes of heterogeneous multi-robots, such as a car and a UAV). Several approaches are proposed to overcome the opposite viewpoint problem. LoST [14] uses semantics and appearance information to recognize the places in the opposite viewpoint. In [15], the place recognition in the opposite viewpoint is handled by matching a sequence of depth-filtered keypoints with a single-query image’s keypoints. However, these approaches are only focused on place recognition; the localization is not considered.

B. Graph-based Approaches

Graph-based methods formulate the global localization problem as a graph registration problem. The associations between different graphs are found by extracting the correspondences between nodes across the graphs. Then, the relative pose between graphs can be calculated.

The key problem of graph-based methods is how to generate the label for each node. Traditionally, they are extracted from appearance information. In [16], [17], each node is labeled by local features based visual word. However, as mentioned before, the appearance features are not reliable when the viewpoint changes are significant.

Recently, several methods employ semantics to generate labels [11], [18]. In [18], brute force is used to match two graphs based on their semantic labels. Unfortunately, this method can only work for simple and limited environments where the number of objects and the environments’ scale are small. The same problem also exists in [11], in which semantic graphs are matched with the Hungarian algorithm. In large scale environments, the same objects frequently appear in multiple places, such as cars and buildings in city blocks. Such environments will lead these methods to fail. To enable more accurate semantic based matching, Random Walk method is used to generate descriptor for each semantic node [9], [10]. However, when the matching graphs are large, the computational complexity becomes extremely high. This will largely hinder the deployment of these methods to real-world applications such as multi-robot SLAM. In this paper, we present a semantic histogram based descriptor, which enables the graph matching to be performed in real-time and it is even more accurate compared to Random Walk based methods.

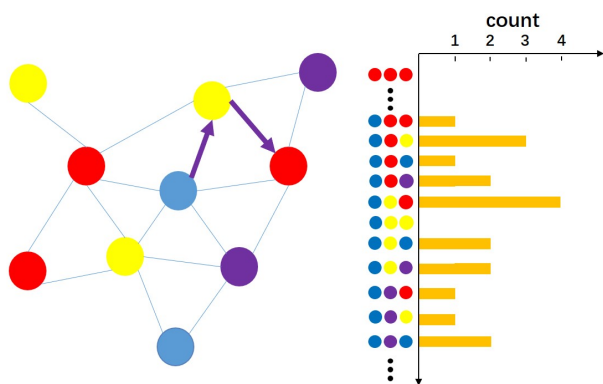


Fig. 2. An illustration of the semantic histogram based descriptor. Left is the semantic graph. The searched path is started from the start point (blue). The path information is recorded as a prearranged histogram on the right. The similarity score between two descriptors can be obtained through the normalized dot-product.

In large scale environments, there will be many mismatches if we directly perform graph matching with only the semantic label of each node. Hence, for each node, the descriptor should be extracted to contain the surrounding information. In the previous methods [9], [10], the Random Walk based descriptors are utilized for graph matching. On the other hand, no matter how large the graphs are, the graph matching needs to be processed in real-time. This requirement eliminates those Random Walk based descriptors [9] [10], which are highly time-consuming.

In this paper, we propose a more accurate and computationally efficient method. Our method is based on the semantic-based graph matching. A novel semantic histogram based descriptor is proposed to enable a real-time matching under the large viewpoint changes. The descriptor stores the surrounding paths’ information in the form of a prearranged histogram. Fig. 2 shows the illustration of the descriptor. Based on the new descriptor, we further develop a semantic graph-based global localization system to merge maps for MR-SLAM. Our method is fairly tested on three datasets, including two synthesized datasets and a publicly available real-world dataset. As a result, we show through the experiments that

- Our method outperforms both appearance and semantic based methods by a large margin. It performs stably and accurately for large viewpoint differences in large scale environments.
- Our method is much faster than the state-of-the-art semantic based method [9]. It yields satisfactory performance for both homogeneous and heterogeneous robot systems.
- Our method demonstrates good performance for map fusion in large scale real-world KITTI dataset in which we only take RGB images as input, the depth maps and semantic maps are predicted by deep convolutional networks.

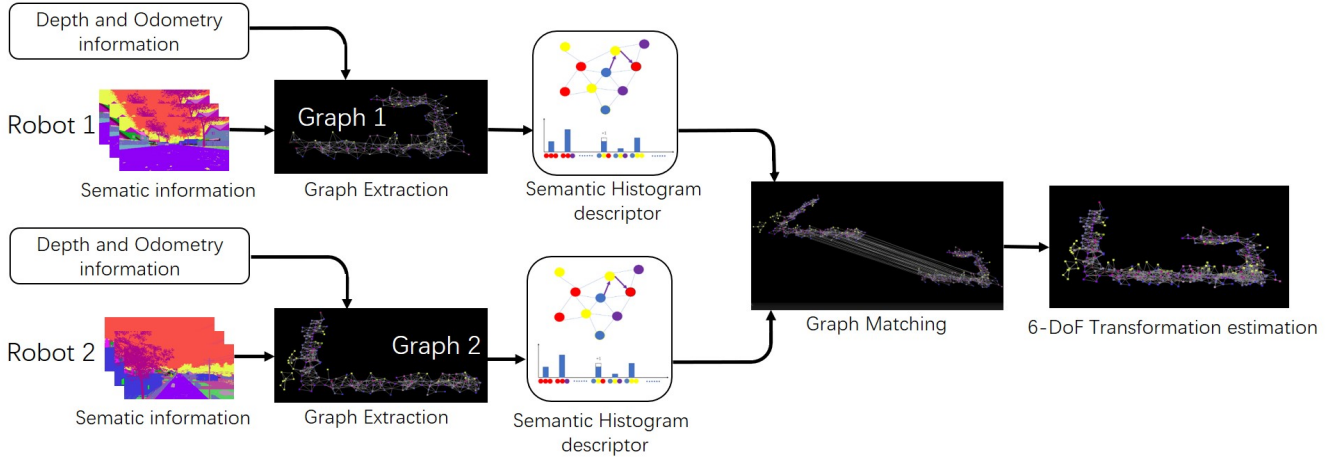


Fig. 3. The diagram of our global localization system. The system takes semantic maps, depth maps, and odometries as inputs. The 3D semantic graph for each robot is first built from the inputs. Then, the descriptor of each node is extracted with the semantic histogram method. Next, the two graphs are matched by comparing the descriptors across the graphs. Finally, the matched correspondences are used to estimate the 6-DoF transformation between the coordinate systems of two robots.

III. SEMANTIC GRAPH-BASED GLOBAL LOCALIZATION

In this section, we present our semantic histogram based graph matching system for global localization. Firstly, given two odometries, related depth maps, and semantic maps. We first generate semantic graphs. Then, the semantic histogram based descriptors are extracted. The two graphs are matched with the extracted descriptors. Finally, the 6-DoF transformation matrix is calculated. The framework of our global localization system is shown in the Fig. 3.

A. Graph Extraction

To build the graph, we need to extract nodes from images. Towards this end, objects in the images are segmented by using the seed filling method. To avoid the failed segmentation between two neighboring objects with the same semantics, we use the 3D coordinates of pixels during the segmentation process. Then, the 3D geometry center of each object is extracted as a node. It's noted that nodes with the same semantic label should be merged if they are highly close to each other. Therefore, each node contains two types of information: 1, 3D coordinates value of the node; 2, The semantic label.

The undirected edges between the nodes are then formed if the distances between nodes are smaller than a set threshold. Finally, nodes and edges together consist of the semantic based graph.

B. Semantic Histogram Based Descriptor

In order to describe each node in the graph, the surrounding information of the node needs to be recorded by extracting the node's descriptor. For the semantic graph, histogram based descriptors are simple and feasible; furthermore, the matching procedure of this type of descriptors is very fast. Intuitively, the simplest histogram based descriptor is the neighbor vector descriptor [17]. It describes the node by

Algorithm 1 Descriptor Extraction

Input: G : Semantic Graph;

Output: V : Histogram of path descriptors for G ;

```

1: for  $i$ -th node in  $G$  do
2:   Initialize the histogram vector  $V_i$ ;
3:   Record the node's label  $l_i$ ;
4:   for  $m$  in neighbor nodes of  $i$  do
5:     Record the first neighbor node's label  $l_m$ ;
6:     for  $n$  in neighbor nodes of  $m$  do
7:       Record the second neighbor node's label  $l_n$ ;
8:       The Histogram cell  $V_i(l_i-l_m-l_n)$  plus one;
9:     end for
10:  end for
11:  Add  $V_i$  into  $V$ ;
12: end for

```

counting all the neighbor nodes' labels. However, due to the lack of topology information, the matching performance of the neighborhood vector is low ¹.

Therefore, we propose to include more surrounding information for all nodes. To be specific, for each node, the descriptor stores all possible paths that started from it. We set the length of the path as 3. Therefore, each path can be considered as a 3-dimensional vector, recording the three steps' semantic labels. For a single descriptor, all possible paths are counted in the form of the prearranged histogram. Therefore, the topology information of objects and their neighbors are stored in descriptors. The illustration of our descriptor is shown in Algorithm 1. The proposed descriptor enables the graph matching to be much computationally efficient.

¹We will confirm this through our experiments evaluations in Sec. IV-B and Sec. IV-C.

Algorithm 2 Graph matching and ICP-RANSAC rejection

Input: V, V' : descriptor sets of two graphs; N_i : iteration number for RANSAC; M_0 : initial matches set;

Output: M_1 : final matches set;

```
1: Initialize  $M_0$ ;
2: for  $i$  in  $V$  do
3:   for  $j$  in  $V'$  do
4:     scores = Score( $V_i, V'_j$ );
5:     if scores > score threshold  $T_s$  then;
6:       Add the Correspondence  $C_{ij}$  to  $M_0$ ;
7:     end if
8:   end for
9: end for
10: Initialize  $M_1$ ;
11: Initialize the Maximum Inlier number  $A^*$ ;
12: let  $A^* = 0$ ;
13: for  $o = 1$  to  $N_i$  do
14:   Select 4 correspondences  $M_{four}$  Randomly;
15:    $R_o, t_o = \text{ICP}(M_{four})$ ;
16:   for  $k$  in Matches set  $M_0$  do
17:     Obtain the correspondence  $C_k$ ;
18:     Error = Evaluation( $C_k, R_o, t_o$ );
19:     if Error < Threshold  $T_R$  then
20:       Add  $C_k$  to the Inlier set  $M_o$ ;
21:     end if
22:   end for
23:   Inlier number  $A = \text{Count}(M_o)$ ;
24:   if  $A > A^*$  then
25:      $M_1 = M_o$ ;
26:      $A^* = A$ ;
27:   end if
28: end for
```

C. Graph Matching

Similar to image matching, the descriptors are compared across the graphs by computing the similarity scores. In the matching process, only the nodes that have the same labels will be compared. The similarity score is obtained by taking the normalized dot-product between two descriptors. It is formulated as follows:

$$\text{Score}(A, B) = \frac{\sum_{d=1}^{n_d} A_d \times B_d}{\sqrt{\sum_{d=1}^{n_d} (A_d)^2} \times \sqrt{\sum_{d=1}^{n_d} (B_d)^2}} \quad (1)$$

Where A and B denote descriptors of two graphs. n_d is the descriptor dimension, which is equal to the cubic of the label number n_l . The time complexity of one pair nodes' matching is $O(n_d)$, the size of the n_d is typically on the order of hundreds.

The similarity scores between the two descriptors are between 0 and 1. The higher scores mean higher similarity. The correspondences whose similarity scores are higher than the threshold T_s are stored as the matching candidates. In order to guarantee the consistency of the correspondences, the outliers are then rejected by using the ICP-RANSAC algorithm [19], [20]. Finally, the remained inlier correspondences are kept

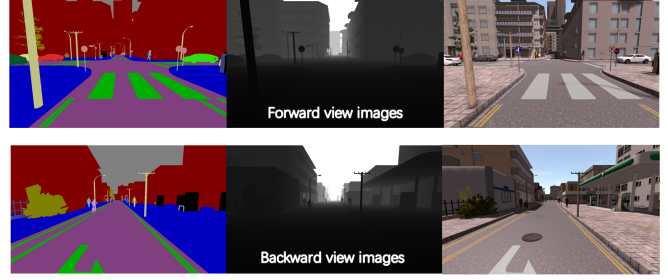


Fig. 4. Samples of SYNTHIA dataset. images in top row are the forward view images, including semantics, depths, and RGB images. The images in bottom row are the backward view images collected at the same time.

for the pose estimation method. In addition, the rotation matrix R and the translation vector t , which are obtained from the ICP-RANSAC method are stored as the initial value of the pose estimation method. The illustration of the graph matching is shown in the Algorithm 2.

D. Pose Estimation

In this step, the final transformation matrix is computed with ICP algorithm. However, In the method, the correspondences is not obtained by matching the closest points. The inlier correspondences obtained by RANSAC method are used for alignment. Hence, the Rotation matrix R and translation vector t is obtained by minimize the sum of squared error:

$$E(R, t) = \frac{1}{N_p} \sum_{k=1}^{N_p} W_k \|q_k - Rp_k - t\|^2 \quad (2)$$

The N_p is the correspondences number after RANSAC rejection. q_k and p_k are the correspondent nodes in two graphs. W_k is the weight element, which is related to the corresponding objects' size.

IV. EXPERIMENT RESULTS

To fairly and fully validate the effectiveness of our method, we conduct three experiments on multiple datasets. First, we show the quantitative comparisons between our method and previous approaches on the SYNTHIA dataset [21]. Second, we show the performance of our method for multi-robot global localization, we apply our method to both homogeneous and heterogeneous multi-robot systems. Finally, to verify the generability of our method, we conduct another experiment on the real-world KITTI dataset, where we only use RGB images as input. All the experiments are computed on an Intel Core i7-8565U CPU @ 1.80GHz.

A. Performance Comparison

1) *Dataset and Implementation Details:* The SYNTHIA dataset collects data from sensors mounted on a simulated car in a dynamic urban environment. It contains three types of data, including RGB images, depth maps, and semantic maps. All these images have four camera directions, i.e., forward, backward, leftward, and rightward. In order to simulate the viewpoint variation, data of the forward view is

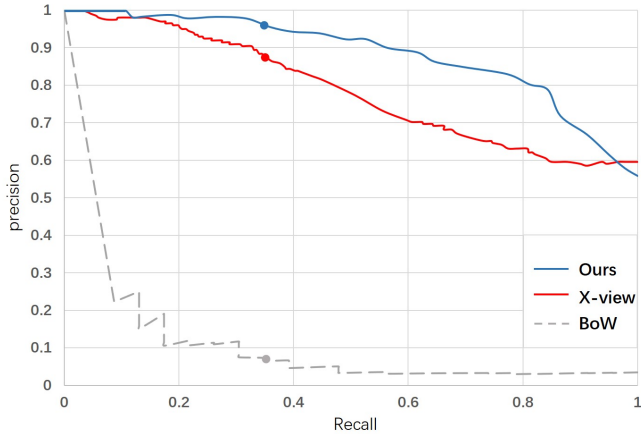


Fig. 5. Precision-Recall curve of different global localization methods. The operation points are shown as dots.

picked to be associated with backward view’s data, as seen in Fig. 4. The travel distance of the dataset is 950 meters.

Two previous methods are taken as baseline methods. The first is X X-view [9], which is the state-of-the-art of semantic graph-based global localization. The second is an appearance-based Bag-of-Words (BoW) method that is built on the DBow3 library [1]. Since there is no available open source code of X-view, we directly use the results in its paper [9] for the comparison. In order to have the fair comparison, the experiment condition and setting are completely consistent with X-view.

2) *Experiment Result:* In the experiment, the performance of the localization is represented by the Precision-Recall curve (PR-curve). The precision depends on the localization threshold $T_p = 20m$. The localization is set to true if the translation error is lower than 20m. The recall is controlled by the variable threshold of T_r . If the inlier number obtained from the ICP-RANSAC method is higher than T_r , then this localization gets a positive vote.

The results are shown in Fig. 5, it’s clear that the semantic graph-based method is more accurate than the appearance-based method when the viewpoint change is significant. Moreover, our method shows a clear advantage against X-view as it outperforms it by a large margin. To be consistent with X-view, we use the same operation point (recall is 0.35) to compare the success rate of global localization; as a result, our method gained 95% success rate while the success rate of BoW and X-view are 8% and 85%, respectively.

B. Global Localization for Multi-robots

1) *Dataset and Implementation Details:* We consider yet another problem that has not been explored in previous studies [9], [10], that is the global localization for multiple large scale odometries generated by multiple robots (also referred to as data association). This is a key step for map fusion of multi-robot SLAM. We evaluate the performance of our method for both heterogeneous and homogeneous robot systems.

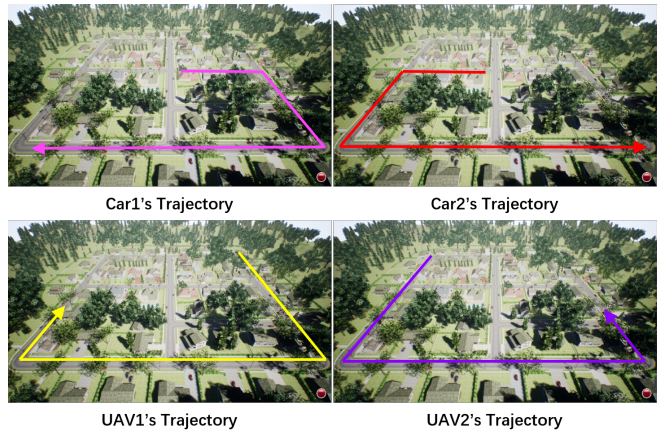


Fig. 6. The illustration of four simulated trajectories generated from AirSim. We use them to evaluate the performance of our global localization method for both homogeneous and heterogeneous robot systems.

As there’s no publicly available dataset for this purpose, we manually create a dataset ² from the Neighborhood (an urban block) of AirSim [22]. Same as the SYNTHIA, the dataset contains three types of data, i.e. RGB images, depth maps, and semantic maps. In order to simulate the scenarios for both heterogeneous and homogeneous robot systems, the dataset is collected from two different robots (a UAV and a Car). For each robot, we generate two different trajectories. Therefore, there are four trajectories in total. The average travel distance of Car is 420 meters, while the average travel distance of the UAV is about 600 meters. The viewpoint change between them is extremely large. The detailed illustrations of these trajectories are shown in figure 6. It’s seen that the different trajectories contain long overlapping parts (over 200 meters); meanwhile, they have their own non-overlapping parts.

There are three descriptors compared in the experiment. The first one is the Random Walk, which is used in X-view. The second one is a fast matching descriptor called Neighbor Vector [17]. The final one is our semantic histogram based descriptor. The matching performance is evaluated by using good matches number and good matches rate. The good match is that the distance between the corresponding nodes is lower than 10 meters. The good match rate is the percentage of the correct matching correspondences represented in the total correspondences.

2) *Experiment Result:* We show the comparisons of global localization for both heterogeneous and homogeneous robot systems. As there are four different trajectories in our dataset, hence, we have 6 different combinations of them in total. The results are shown in Table I, where we show the processing time (from descriptor extraction to pose estimation) and translation error (100 times’ average). For detailed comparisons between different descriptors, the matching performance is also given.

As shown in the table, for all scenarios, our descriptor’s matching performance is the highest. Furthermore, it’s clear

²The dataset will be made publicly available.



Fig. 7. Visualization of fused maps for homogeneous and heterogeneous robot systems. Left shows the fused maps for homogeneous robots (Car1 and Car2), right shows the fused maps for heterogeneous robots (Car1 and UAV2).

TABLE I
THE QUANTITATIVE COMPARISONS OF DIFFERENT DESCRIPTORS FOR GLOBAL LOCALIZATION OF MULTI-ROBOT SYSTEMS ON AIRSIM.

Robot Type	Matching Graph Size	Descriptor Type	Matching Time (sec)	Good Matches	Good Matches Rate(%)	Processing Time (sec)	Translation Error (m)
Car1 and Car2	317 points and 328 points	Random Walk and Neighbor Vector	4.155	125	40.0	4.304	3.44 ± 1.39
		Ours	0.013	120	37.8	0.057	4.55 ± 1.32
			0.132	152	49.1	0.184	3.12 ± 0.76
UAV1 and UAV2	370 points and 486 points	Random Walk and Neighbor Vector	8.530	132	36.5	8.769	2.46 ± 1.27
		Ours	0.024	105	28.6	0.097	7.65 ± 4.26
			0.224	146	40.0	0.282	2.09 ± 0.45
Car1 and UAV1	317 points and 370 points	Random Walk and Neighbor Vector	5.598	165	53.0	5.781	2.95 ± 0.27
		Ours	0.014	123	38.4	0.072	3.55 ± 1.23
			0.144	167	53.2	0.206	2.68 ± 0.31
Car1 and UAV2	317 points and 486 points	Random Walk and Neighbor Vector	6.637	136	43.6	6.859	2.23 ± 0.88
		Ours	0.021	100	31.7	0.089	3.23 ± 1.02
			0.195	142	45.1	0.248	2.12 ± 0.47
Car2 and UAV1	328 points and 370 points	Random Walk and Neighbor Vector	5.342	110	34.3	5.524	3.55 ± 1.27
		Ours	0.015	88	26.2	0.084	4.26 ± 1.43
			0.148	113	34.8	0.196	2.59 ± 0.89
Car2 and UAV2	328 points and 486 points	Random Walk and Neighbor Vector	7.220	127	39.4	7.448	1.59 ± 0.70
		Ours	0.021	115	35.5	0.095	1.61 ± 0.35
			0.202	134	41.4	0.261	1.42 ± 0.39

that our method achieves the lowest translation error for global localization. The average error of Random Walk, Neighbour Vector, and our semantic histogram method is 2.70, 4.14, and 2.34 meters, respectively. The lowest translation error of our method is attributable to the highest good matches rate, as shown in the Table I.

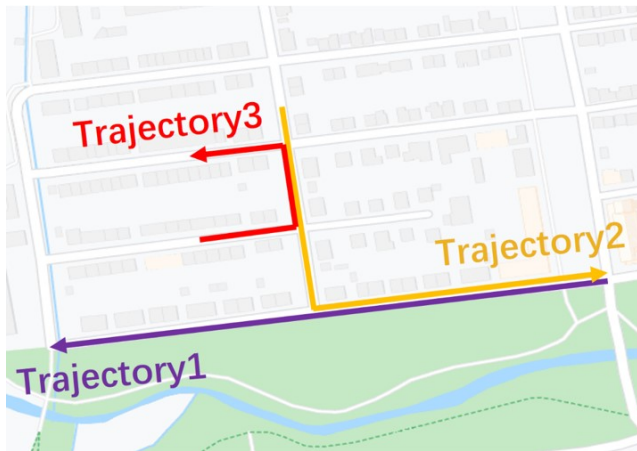
By considering the time complexity, the Neighbor Vector descriptor has the lowest time complexity. However, due to the less surrounding information, the matching performance of the Neighbor Vector is the worst. The time complexity of our descriptor is higher than Neighbor Vector but much lower than the Random Walk. Hence, by considering the trade-off between matching performance and time complexity, our descriptor is the best for semantics graph matching. Overall, our method demonstrates the best performance for the large viewpoint difference between both heterogeneous and homogeneous robot systems. The visualization of map fusion after applying our global localization method is shown in Fig. 7. The map is consists of the dense point cloud with semantic information.

C. Generability on Real-World Scenarios

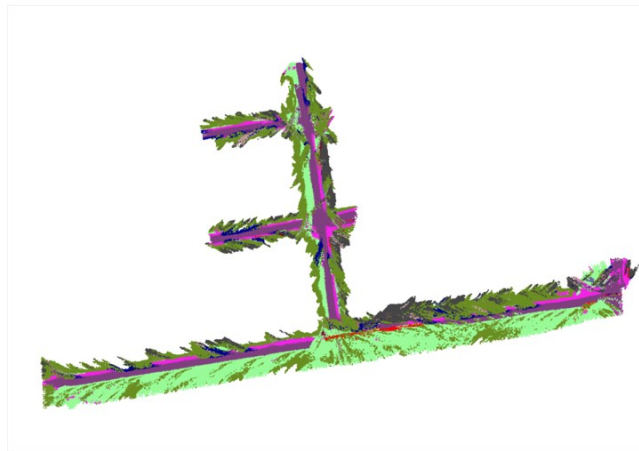
1) *Dataset and Implementation Details:* To evaluate the generability of our method in real-world environments, we conduct yet another experiment on the KITTI dataset [23]. To be specific, we evaluate our method on sequence 08 of the KITTI odometry benchmark. In the experiment, three trajectories are split from the sequence. The illustration of the three trajectories are shown in Fig. 8 (a). The total length of the trajectories is 850 meters. The overlap between Trajectory1 and Trajectory2, Trajectory2 and Trajectory3 is 200 meters and 50 meters, respectively.

As the dataset only contains RGB images, there are no ground truths of depth maps and semantic maps. Therefore, we apply current advanced algorithms to estimate depth maps and semantic maps, respectively. The depths are predicted with the method of [24], and the semantics are estimated with [25]. For odometry estimation, we use ORB-SLAM3 [26].

2) *Experiment Result:* Table II shows the average translation errors and their standard deviation on the KITTI



(a) The trajectories of KITTI dataset



(b) The successful multi-robots map fusion

Fig. 8. Trajectories and reconstructed maps of KITTI dataset. a) shows the trajectories where each line denotes a trajectory. b) shows the maps reconstructed and merged from these three trajectories.

TABLE II
THE TRANSLATION ERROR OF GLOBAL LOCALIZATION ON THE KITTI DATASET

Trajectories	Overlap(m)	Descriptor type	Processing Time(sec)	Translation error(m)
Trajectory1 and Trajectory2	200	Random Walk	15.542	4.83 ± 0.68
		Neighbor Vector	0.157	4.59 ± 0.63
		Ours	0.408	4.45 ± 0.35
Trajectory2 and Trajectory3	50	Random Walk	3.655	25.55 ± 8.72
		Neighbor Vector	0.060	18.42 ± 4.00
		Ours	0.123	7.48 ± 3.67

dataset. According to the table, our semantic histogram based descriptor archives 4.45 ± 0.35 meters translation error which is slightly better than Random Walk and Neighbor Vector when the overlap is 200 meters, it's noted that when the overlap is small, our method shows the clear advantage against others. As seen in the table, when the overlap is 50 meters, the translation error is 7.48, 25.55, and 18.42 meters for our method, Random Walk and Neighbor Vector, respectively. The advantage of our method is significant. By considering the threshold (< 20 meters) of translation error, only Neighbor Vector and our method can successfully perform global localization.

As indicated by the results, the translation error is obviously large than those on AirSim. This is because of the unavoidable error of depth and semantic prediction with deep neural networks. Another intriguing observation is Random Walk based descriptor is worse than Neighbor Vector on the KITTI dataset, which is not consistent with the results on AirSim. Due to the higher quantity of objects and misclassification problem, the semantic graphs of KITTI contain higher nodes density. The higher nodes density brings more possibilities of walks. Then, the Random Walk descriptor is easier to omit the possible walks. Therefore, the performance of Random Walk descriptor is dropped significantly. By considering the unstable performance of these methods, our method performs robustly and accurately for both synthesized and real-world scenarios.

Fig. 8 (b). shows the visualization of map fusion after the

global localization performed by our system. Same as the AirSim, the maps are generated by the dense point cloud with the semantic information.

V. CONCLUSIONS

In this paper, we studied the problem of global localization for vision based multi-robot SLAM. We argue that there are mainly two difficulties that need to be well handled. The first is the large viewpoint difference, which is ubiquitous for multi-robot systems. In large scale environments such as urban scenarios, the viewpoint between robots are dramatically different, the difference is more significant for heterogeneous robot systems. However, previous appearance-based methods tend to fail for such a large viewpoint difference. The second difficulty is the global localization needs to be performed in real-time. It is crucial for the subsequent map fusion step of multi-robot SLAM. This requirement immediately eliminates the state-of-the-art Random Walk based semantic method, which is highly time-consuming.

The above difficulties motivated us to develop a more effective and efficient method for global localization. In this paper, we proposed a semantic histogram based descriptor. Thanks to that, the graph matching is formulated as a dot-product between two descriptor sets, which can be performed in real-time. Based on the proposed descriptor, we presented a more accurate and efficient global localization system. The system is fairly tested on synthesized SYNTHIA and AirSim datasets. The experimental results show that our

method outperforms others by a good margin, and it is much faster than the previous semantic based method built on the Random Walk. To evaluate the generability of our method for real-world environments, we conduct another experiment on the real-world KITTI dataset. The results agree well with comparisons between the results of the proposed method and those of the previous ones on the synthesized datasets.

REFERENCES

- [1] D. Galvez-López and J. D. Tardos, “Bags of binary words for fast place recognition in image sequences,” *IEEE Transactions on Robotics*, vol. 28, no. 5, p. 1188–1197, 2012.
- [2] M. Cummins and P. Newman, “Fab-map: Probabilistic localization and mapping in the space of appearance,” *The International Journal of Robotics Research*, vol. 27, no. 6, p. 647–665, 2008.
- [3] P. Schmuck and M. Chli, “Multi-uav collaborative monocular slam,” *2017 IEEE International Conference on Robotics and Automation (ICRA)*, 2017.
- [4] X. Chen, H. Lu, J. Xiao, and H. Zhang, “Distributed monocular multi-robot slam,” *2018 IEEE 8th Annual International Conference on CYBER Technology in Automation, Control, and Intelligent Systems (CYBER)*, 2018.
- [5] D. G. Lowe, “Distinctive image features from scale-invariant keypoints,” *International Journal of Computer Vision*, vol. 60, no. 2, p. 91–110, 2004.
- [6] H. Bay, A. Ess, T. Tuytelaars, and L. V. Gool, “Speeded-up robust features (surf),” *Computer Vision and Image Understanding*, vol. 110, no. 3, p. 346–359, 2008.
- [7] E. Rublee, V. Rabaud, K. Konolige, and G. Bradski, “Orb: An efficient alternative to sift or surf,” *2011 International Conference on Computer Vision*, 2011.
- [8] E. Rosten and T. Drummond, “Machine learning for high-speed corner detection,” *Computer Vision – ECCV 2006 Lecture Notes in Computer Science*, p. 430–443, 2006.
- [9] A. Gawel, C. D. Don, R. Siegwart, J. Nieto, and C. Cadena, “X-view: Graph-based semantic multi-view localization,” *IEEE Robotics and Automation Letters*, vol. 3, no. 3, p. 1687–1694, 2018.
- [10] Y. Liu, Y. Petillot, D. Lane, and S. Wang, “Global localization with object-level semantics and topology,” *2019 International Conference on Robotics and Automation (ICRA)*, 2019.
- [11] J. Li, D. Meger, and G. Dudek, “Semantic mapping for view-invariant relocalization,” *2019 International Conference on Robotics and Automation (ICRA)*, 2019.
- [12] N. Suenderhauf, S. Shirazi, A. Jacobson, F. Dayoub, E. Pepperell, B. Upcroft, and M. Milford, “Place recognition with convnet landmarks: Viewpoint-robust, condition-robust, training-free,” *Robotics: Science and Systems XI*, 2015.
- [13] Z. Chen, A. Jacobson, N. Suenderhauf, B. Upcroft, L. Liu, C. Shen, I. Reid, and M. Milford, “Deep learning features at scale for visual place recognition,” *2017 IEEE International Conference on Robotics and Automation (ICRA)*, 2017.
- [14] S. Garg, N. Suenderhauf, and M. Milford, “Lost? appearance-invariant place recognition for opposite viewpoints using visual semantics,” *Robotics: Science and Systems XIV*, 2018.
- [15] S. Garg, M. B. V. T. Dharmasiri, S. Hausler, N. Suenderhauf, S. Kumar, T. Drummond, and M. Milford, “Look no deeper: Recognizing places from opposing viewpoints under varying scene appearance using single-view depth estimation,” *2019 International Conference on Robotics and Automation (ICRA)*, 2019.
- [16] E. Stumm, C. Mei, S. Lacroix, and M. Chli, “Location graphs for visual place recognition,” *2015 IEEE International Conference on Robotics and Automation (ICRA)*, 2015.
- [17] E. Stumm, C. Mei, S. Lacroix, J. Nieto, M. Hutter, and R. Siegwart, “Robust visual place recognition with graph kernels,” *2016 IEEE Conference on Computer Vision and Pattern Recognition (CVPR)*, 2016.
- [18] R. Finman, L. Paul, and J. L. Leonard, “Toward object-based place recognition in dense rgb-d maps,” *ICRA Workshop on Visual Place Recognition in Changing Environments*, 2015.
- [19] P. J. Besl and N. D. McKay, “Method for registration of 3-d shapes,” in *Sensor fusion IV: control paradigms and data structures*, vol. 1611. International Society for Optics and Photonics, 1992, pp. 586–606.
- [20] M. A. Fischler and R. C. Bolles, “Random sample consensus: a paradigm for model fitting with applications to image analysis and automated cartography,” *Communications of the ACM*, vol. 24, no. 6, pp. 381–395, 1981.
- [21] G. Ros, L. Sellart, J. Materzynska, D. Vazquez, and A. M. Lopez, “The synthia dataset: A large collection of synthetic images for semantic segmentation of urban scenes,” *2016 IEEE Conference on Computer Vision and Pattern Recognition (CVPR)*, 2016.
- [22] S. Shah, D. Dey, C. Lovett, and A. Kapoor, “Airsim: High-fidelity visual and physical simulation for autonomous vehicles,” *Field and Service Robotics Springer Proceedings in Advanced Robotics*, p. 621–635, 2017.
- [23] A. Geiger, P. Lenz, and R. Urtasun, “Are we ready for autonomous driving? the kitti vision benchmark suite,” *2012 IEEE Conference on Computer Vision and Pattern Recognition (CVPR)*, 2012.
- [24] J. H. Lee, M.-K. Han, D. W. Ko, and I. H. Suh, “From big to small: Multi-scale local planar guidance for monocular depth estimation,” *arXiv preprint arXiv:1907.10326*, 2019.
- [25] Y. Zhu, K. Sapra, F. A. Reda, K. J. Shih, S. Newsam, A. Tao, and B. Catanzaro, “Improving semantic segmentation via video propagation and label relaxation,” *2019 IEEE/CVF Conference on Computer Vision and Pattern Recognition (CVPR)*, 2019.
- [26] C. Campos, R. Elvira, J. J. G. Rodríguez, J. M. Montiel, and J. D. Tardós, “Orb-slam3: An accurate open-source library for visual, visual-inertial and multi-map slam,” *arXiv preprint arXiv:2007.11898*, 2020.